The application of numerical methods for the solution of some problems in free-surface hydrodynamics

U. Bulgarelli
up.bulgarelli@insean.it

INSEAN, Italian Ship Model Basin, Roma – Italy.

The objective of this paper is to present a survay of some recent accomplishments in accurate and robust algorithm development for the solution of complex free surface flows governed by partial differential equations.

In the quest for accurate numerical methods for time-dependent nonlinear free surface flow, a first, decisive step was taken by Longuet-Higgins and Cokelet (1976) that demonstrated the possibility of computing an overturning wave. Since then, the concept of *numerical wave tank* has evolved as a plethora of numerical methods for the simulation of nonlinear free surface and floating body motions that would make the hydrodynamic analysis of marine vessels in arbitrary sea conditions possible, in a way much similar to what envisioned in a paper by Chapman, Mark and Pirtle (1975) in which the concept of *numerical wind tunnel* was firstly introduced.

This vision has been partially accomplished in principle, although, in practice, some important issues remain to be solved. Recent developments however allow for accurate simulations of 2D and 3D flows even in the presence of large free-surface deformations. This paper describes INSEAN contribution in the development of these numerical methods.

Sloshing

Sloshing is a resonance phenomenon inside partially filled tanks where the free-surface can highly deform. Resulting slamming loads are of main concern and require the use of robust and accurate techniques. The approach adopted is based on the SPH method by Colagrossi and Landrini (2003). Here we analyze the 2D flow in the rigid square tank sketched in figure 1. The main tank dimensions are $L = H = 1$ m. The used geometry is simple enough to allow a systematic

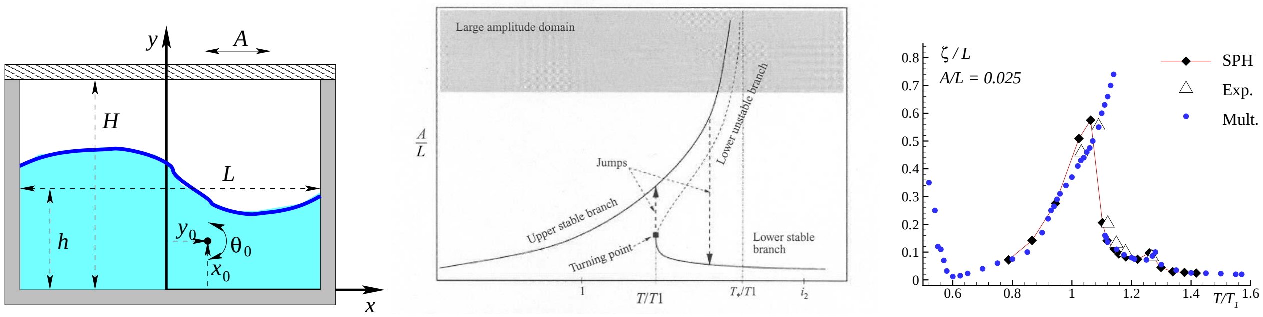

Figure 1: Sloshing in a square tank. Left: sketch of the problem. Center: the 'soft spring' type amplitude response from the modal theory by Faltinsen *et al.* (2000). $h > h^* = 0.337L$. Right: maximum wave height as a function of the excitation period, for the forced sway motion. $A = 0.025L$ and $h = 0.35L$.

investigation of the sloshing events. Here, forced pure-sway motions ($x = A\sin(2\pi t/T)$) and forced pure-roll motions ($\theta = \theta_0 \sin(2\pi t/T)$) are discussed. Experiments on forced roll and sway are available from Olsen (1970) and model tests on forced sway are currently under development at INSEAN (tank width $b = 0.1$ m, Colagrossi *et al.* (2004)). Sloshing features and related dominant modes depend on the excitation amplitude (A or θ_0, see figure 1) and period (T) and on the filling water height (h) inside the tank. The single dominant modal method by Faltinsen *et al.* (2000) shows the existence of a critical water depth, $h^* = 0.337L$. For $h > h^*$, the (steady-state) amplitude of the dominant mode behaves as reported in the center plot of figure 1. A solution bifurcation is observed in the vicinity of primary resonance of the

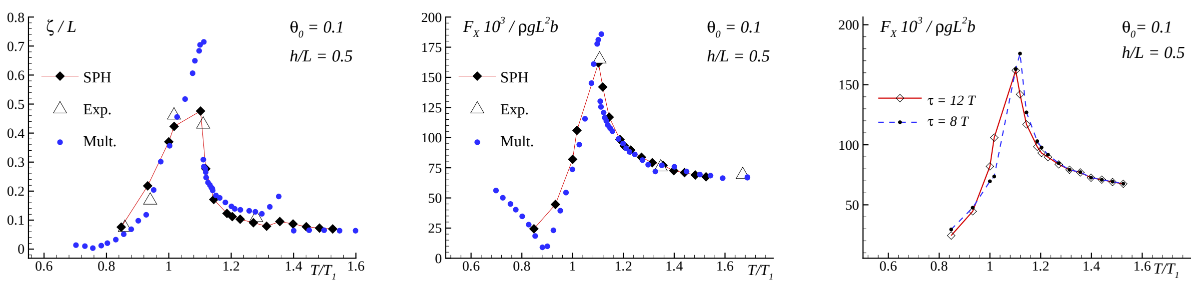

Figure 2: Sloshing in a square tank: forced roll motion. Left: maximum wave height as a function of the excitation period. Center: amplitude of the lateral force F_x. Right: effect of initial ramp τ on the SPH F_x. $\theta_0 = 0.1$ and $h = 0.5L$.

dominant mode. Different branches exist and the solution can jump from one stable branch to another one. The transient conditions will determine the actual branch for the steady–state solution. The result shown is valid also when more than one mode is dominant, as it is likely to happen in reality. This is confirmed by right plot of figure 1. There the maximum wave height (ζ) in the tank is reported as a function of the excitation period, for forced sway motion with $A = 0.025L$ and

$h = 0.35L$. The ζ-curve shows jumps in the solution near the primary resonance of the first mode and near the secondary resonance of the second mode. The SPH calculations compare well with the analytically oriented multi-modal method by Faltinsen *et al.* (2000), and with Olsen's experiments. The more analytical approach is robust and efficient and allows for a better understanding of the sloshing flow regimes and for guiding the development of the used CFD code. However, it cannot handle free-surface breaking, roof impacts and bubbly flows which are practically relevant and ask for a proper modeling. Left and center plots of figure 2 give, respectively, the maximum wave amplitude and the horizontal force, for forced roll motion with $h = 0.5L$ and $\theta_0 = 0.1$ rad. The results agree globally but the multi-modal method can not predict the roof impacts observed by SPH and model tests. The $zeta$-curve has jumps similarly to the sway case. The multi-modal method predicts two jumps, while the SPH results show only one jump near the first resonance period. The SPH simulations have been performed with an initial transient phase. This seems not relevant for the sloshing results at least within the chosen range of ramp duration, as confirmed for instance by the results for F_x in the right plot of figure 2. The different jump behavior between the multi-modal and SPH results requires further investigation.

Water on deck

The water on deck is another relevant problem for ship hydrodynamics and represents a danger for safety and operability of the vessels, independently of their specific type. Differently from the sloshing problem, Boundary Element Methods (BEM) can be applied more extensively in this problem. In the case of bow-deck wetness in head sea conditions, compact masses of water may invade the ship deck, propagating similarly to the flow generated after the breaking of a dam. The water can hit superstructures on its way and t can cause relevant structural loads. Due to the observed similarities, the dam-breaking *plus* impact problem is often studied to develop proper water-on-deck methods. Here the 2D case sketched in the left plot of figure 3 is analyzed. A reservoir of water high H and long $L = 2H$ is closed by a

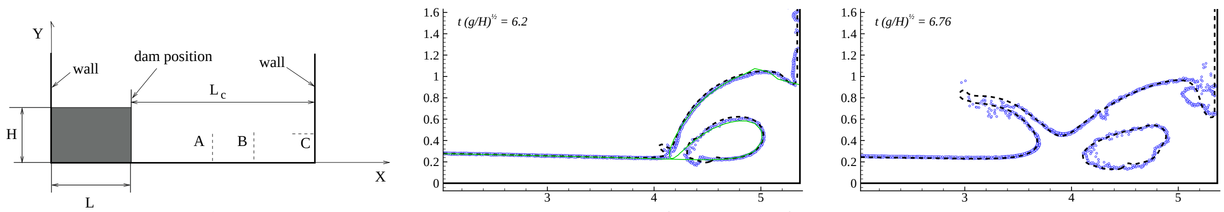

Figure 3: Dam-break flow and impact against a vertical wall. Left: sketch of the problem. Center and right: BEM (solid line), SPH (dots) and Level-set (dashed line) free surfaces at $t\sqrt{g/h} = 6.2$ and 6.76.

dam suddenly released at $t = 0$. Then, the liquid flows and eventually hits a vertical wall $3.366H$ downstream the initial dam. Due to the impact, the water rises up onto the wall. Later the gravity causes its fall down. This leads to a backward plunging wave impacting onto the underlying water, center plot of the figure. BEM (Greco (2001)), SPH (Colagrossi and Landrini (2003)) and Level-set (Colicchio *et al.* (2002)) free-surface results compare well. After the water-water impact, the BEM solution is not available. The used field methods confirm a good agreement for both the developing splash-up and the air cavity caused by the impact (right plot). Left plot of figure 5 gives the pressure evolution on the vertical wall as obtained by the three methods and experimentally (Zhou *et al.* (1999)). The results are globally in a fair agreement. The pressure shows two relevant peaks. The first one is related to the initial water-wall impact, and could be predicted by analytic oriented methods. The second one is connected with the impact of the later backward plunging wave. In this case the use of field methods is requested but still further studies are needed, as confirmed by the post-impact pressure phase showing the largest discrepancies among toe numerical methods and the experiments.

Heterogeneous unsteady domain decomposition approach for breaking waves

Even if free surface capturing models, able to deal with a substantial two-phase flow have been developed and are now at hand, the cost of a detailed computation of the breaking and post-breaking evolution is still very high. This motivated the development of an unsteady heterogeneous domain decomposition approach (DD) (Iafrati and Campana (2003)) to study the wave breaking flow induced by a submerged hydrofoil moving beneath the free surface (see fig. 4).

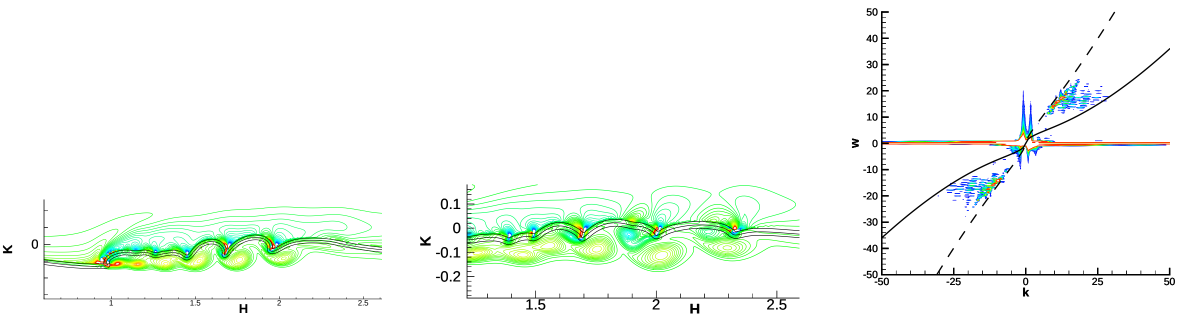

Figure 4: Microscale breaking waves leading to the generation of downstream propagating surface ripples: vorticity field and wavelenght-frequency spectrum are shown

In the free surface region the flow is described with the help of a Navier-Stokes solver coupled with a Level-Set technique for the interface capturing. In the body region a potential flow approximation is used instead and a steady Kutta condition is applied at the trailing edge to account for the lifting effects. With this technique, surface tension effects onto resulting free surface flow have been investigated by Iafrati and Campana (2003). At the micro-breaker lenght scale (see fig. 4) the breaking establishment is characterized by the formation of a bulge about the wave crest which slides upon the forward face of the wave. As a result the air entrapment is suppressed. During the downslope motion of the bulge, an intense shear layer develops from the toe. Shear layer instabilities develops and, when increasing the Reynolds number, they give rise to coherent vortex-structures that interact with the free surface, eventually leading to the formation of large surface fluctuations which propagate downstream.

The spectral analysis reveals that downstream propagating ripples increase their wavelenght while reducing their amplitude. The wavelenght-frequency spectrum, shown in fig. 4, lies within two dispersion relations for gravity-capillary waves, with and without the current effect. Near the breaking region, the fluid is essentially at rest and then the dispersion relation without current effects (solid line in fig. 4) is approached. While propagating downstream, the fluid is progressively accelerated and the dispersion relation with current effects (dashed line) is a upper bound for the spectrum.

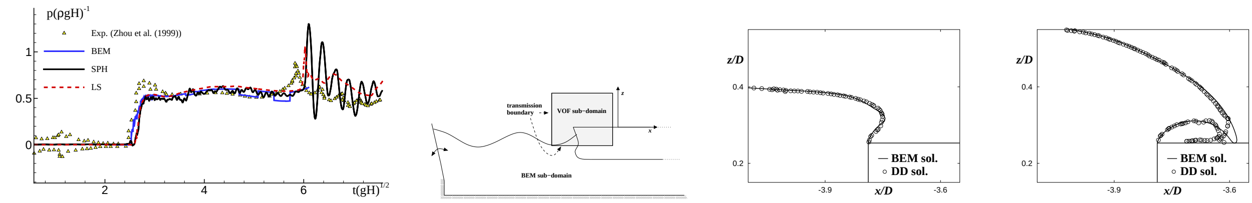

Figure 5: Left: impact against a vertical wall. Pressure evolution on the wall. BEM, SPH and Level-set results and experiments from Zhou *et al.* (1999). Other plots: domain-decomposition strategy for the problem of water on deck on a ship (second from left) and free surface configurations at $t\sqrt{g/D} \simeq$ 55.9 and 56.4 from the starting of the wave-maker motion (two right plots). DD (symbols) and full BEM results (solid lines).

Another relevant DD application is found when the inside ship flow has to be analyzed in connection with the external ship dynamics. In this way the BEM can analyze the flow regions with non-breaking free-surface, while a field method can describe the flow evolution in proximity of the ship bow and on the ship deck. Center and right plots of figure 5 give an example of application of a domain-decomposition strategy applied to the water shipping phenomenon (see the sketch), where a BEM has been combined with a Volume-of-Fluid (VOF) technique. The shown application corresponds to the 2D water on deck experiments reported in Greco (2001). The DD (symbols) free surface evolution is compared with the full BEM solution (solid lines). The results confirm the validity of the DD strategy but suggest the need to improve the VOF treatment here adopted.

Steady breakers generated by a ship

A numerical tool based on the pseudo–compressible Reynolds Averaged Navier Stokes Equations in conjunction with both surface fitting technique (Di Mascio, Broglia and Favini 2001) and a non standard one–phase level set methodology (Di Mascio, Broglia and Muscari 2004) has been developed at the INSEAN to simulate a viscous turbulent flow around a surface piercing ship hull. The use of a level set approach permits the capture steady breakers around the ship. As it is well know, bow wave breaking is one of the main source of air entrainment and consequentially of the so–called white–water wake phenomena; the dispersion of bubbles in water can increase the signature of the ship and reduce the propeller efficiency. As an example, the flow field around the US naval combatant DDG–51 in breaking flow regime is presented. Relevant parameters are Froude and Reynolds numbers, which are equal to 0.41 and 1.85×10^7, respectively. In figure (6) wave profile as well as a three–dimensional view of the wave pattern are shown (the zero level of the level set function is plotted). The capabilities of the proposed algorithm in dealing with breaking flows can be clearly appreciated. Some interesting features of a wavy flow around a ship hull under breaking conditions can be highlighted: at the bow region the water tends to climb along the side wall, with the formation of a thin film of water on the surface of the ship hull. Further downstream, the formation of a jet of water can be observed; after impinging the free surface, a second jet can be clearly noticed. In the close–up views of figure (6) the reconnection phase of the first and second plunging jets is shown.

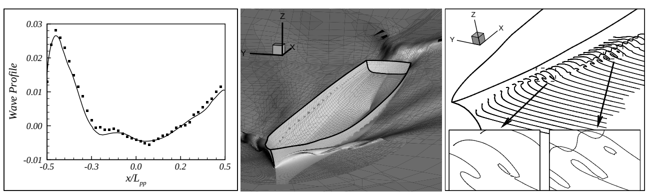

Figure 6: DDG–51 at $Fr = 0.41$–$Re = 1.85\,10^7$. Left: Wave profile along the hull. Numerical results (solid line) vs. experimental data (dots). Center: perspective view of the wave pattern Right: transverse wave cuts.

Unsteady viscous free-surface flow past a ship in forced motion

The correct prediction of the hydrodynamic forces and moments acting on a manoeuvering ship is of great interest for safety and comfort reasons. Analysis of such kind of problems by means of numerical investigation requires *ad hoc* methodologies capable to deal with unsteadiness of the flow field and with the presence of moving bodies. Moreover, in the case of large horizontal plane motions and/or roll motions, effects due to the viscosity and turbulence must be taken into account. The solution of the unsteady incompressible Navier–Stokes equations is obtained by means of a second order multi–block finite volume solver. The algorithm is based on the steady RANS solver developed at the INSEAN (Di Mascio, Broglia and Favini 2001): convective fluxes in the momentum equations are evaluated by means of a second order TVD scheme, whereas diffusive fluxes are discretized by a centered scheme. At the free surface both dynamic and kinematic boundary conditions on the actual position are enforced; the movement of the surface is handled by a surface fitting technique. Physical time-derivative in the governing equations is approximated by a second order accurate, three–point backward finite difference formula. In order to satisfy divergence free velocity field at every physical–time step, a dual or pseudo time–derivative is introduced in the discrete system of equations (Broglia and Di Mascio 2003). Acceleration of the convergence for the inner iteration is achieved by means of an efficient multigrid technique (Favini, Broglia and Di Mascio 1996). Results of the unsteady flow around a Serie–60 ship hull in Zig–Zag manoeuvre are presented: forced motion consists in a combination of a periodical sway and yaw motions with a phase shift of $\pi/4$ and period of four time units. An example of the wave pattern configuration during the Zig–Zag monoeuvre is given in figure 7.

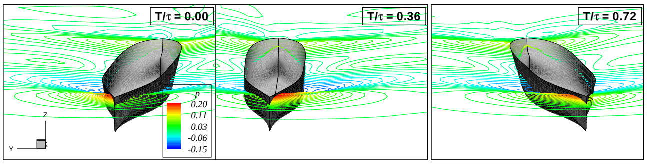

Figure 7: Serie–60 in Zig–Zag manoeuvre ($Fr = 0.316, Re = 4.0\,10^6$). Front view of the wave pattern at three different instant in time during one period of prescribed motion.

References

R. Broglia and A. Di Mascio, 2003, ”Unsteady RANS Calculations of the Flow Around a Moving Ship Hull”, Proc. 8^{th} Int. Conf. on Num. Ship Hydro., Busan, Korea.

D.R. Chapman, H. Mark and M.W.Pirtle, 1975, ”Computer vs. wind tunnels in aerodynamic flow simulation”, Astronautics and Aeronautics, **13** (4), pp. 22-30.

A. Colagrossi and M. Landrini, 2003, ”Numerical Simulation of Interfacial Flows by Smoothed Particle Hydrodynamics”, J. Comp. Phys., **191**, pp. 448-475.

A. Colagrossi, C. Lugni, M. Greco and O.M. Faltinsen, 2004, ”Experimental and numerical investigation of 2D sloshing with slamming”, Proc. 19^{th} Int. Workshop on Water Waves and Floating Bodies, Cortona, Italy.

G. Colicchio, M. Landrini and J. Chaplin, 2002, Level-set Simulation of the Vortical Flow Generated by a Surface-piercing Body, 5^{th} Num. Towing Tank Symp. (NuTTS), Pornichet, France.

A. Di Mascio, R. Broglia and B. Favini, 2001, ”A Second Order Godunov–Type Scheme for Naval Hydrodynamics”, Godunov Methods: Theory and Applications, Kluwer Academic/Plenum Publishers, 253–261.

A. Di Mascio, R. Broglia and R. Muscari, 2004, ”A Single–Phase Level Set Method for Solving Incompressible Viscous Free Surface Flows”, Submitted for publication to Int. J. Numer. Meth. Fluids.

O.M. Faltinsen, O.F. Rognebakke, I.A. Lukovsky and A.N. Timokha, 2000, ”Multidimensional modal analysis of nonlinear sloshing in a rectangular tank with finite water depth”, J. Fluid Mech., 407, 201–234.

B. Favini, R. Broglia, and A. Di Mascio, 1996, ”Multi–grid Acceleration of Second Order ENO Schemes from Low Subsonic to High Supersonic Flows”, Int. J. Numer. Meth. Fluids, 23, 589–606.

M. Greco, 2001, ”A Two-dimensional Study of Green-Water Loading”, Dept. Marine Hydro., NTNU, Trondheim, Norway.

A. Iafrati and E.F. Campana, 2003, ”A domain decomposition approach to compute wave breaking”, Int. J. Numer. Meth. Fluids, **41**, 419–445.

A. Iafrati and E.F. Campana, 2002, ”Direct numerical simulation of surface tension dominated and non-dominated breaking waves”, 24–th ONR Symp. on Naval Hydro., Fukuoka, Japan

M.S. Longuet-Higgins and E.D. Cokelet, 1976, ”The deformation of step surface waves on water. I. A numerical method of computation”, Proc. R. Soc. Lond., A 350, 1–26.

H. Olsen, 1970, ”Unpublished sloshing experiments at the Technical University of Delft”, Delft, The Netherlands.

Zhou Z.Q., De Kat J.O. and Buchner B., 1999, A Nonlinear 3–D Approach to Simulate Green Water Dynamics on Deck, In: Proc. 7^{th} Int. Conf. Num. Ship Hydrod., Nantes, Ed. J. Piquet, pp. 5.1–1, 15.